Defence Science Journal, Vol. 70, No. 6, November 2020, pp. 664-671, DOI : 10.14429/dsj.70.15516

Thermo-mechanical and Control Behaviour of Copper-based Shape Memory Alloy Bimorph Actuator towards the Development of Micro Positioning System

M. Muralidharan[#,*], S. Jayachandran[#], M. Yogeshwaran[@], A.S. Shivaani[@], and I.A. Palani[#]

[#]*Indian Institute of Technology Indore, Simrol - 453 552, India*
[@]*Mechatronics Engineering, Bannari Amman Institute of Technology, Sathyamangalam - 638 401, India*
[*]*E-mail: muralidharanporthy@gmail.com*

ABSTRACT

A shape memory alloy (SMA) bimorph actuator is a composite structure composed of flexible polyimide substrate and SMA thin film deposited using thermal evaporation technique. In this work, the substrate thickness in the range of 25 - 75 μm was selected for the development of CuAlNiMn SMA bimorph actuator. An investigation on the control behavior of copper based SMA bimorph towards the development of micro positioning system has been performed. The actuation behavior of the SMA bimorph was studied using electrical actuation. Subsequently, a proportional integral derivative (PID) controller was designed to control the bimorph actuator with proper tuning of gain parameters. The displacement of the bimorph actuator was controlled through dedicated experimental setup consisted of laser displacement sensor, data acquisition system and LabVIEW software. The CuAlNiMn SMA bimorph actuator resulted in a satisfying control performance which can be extended to MEMS applications. A preliminary prototype of the SMA bimorph actuator based micro positioning system has been developed.

Keywords: Bimorph actuator; Shape memory alloy; MEMS; Mechatronics; Micro positioning; PID control

1. INTRODUCTION

Smart materials have been used widely in the development of micro devices for better performance. Piezoelectric, shape memory alloy (SMA) and ionic polymer composites (IPMC) are the smart materials which have garnered interest in the development of micro actuators[1-8]. Among these smart materials, SMA possesses highest energy density and benefits the development of high performance micro actuators[9-14]. SMA can recover large strain and suitable for the development of micro devices like micro pump, micro wrapper/micro grippers, micro cantilever, micro thermostat array and micro mirror[15-22]. SMA thin film has potential applications as sensors/actuators in the fields of biomedical, MEMS, automobile, military and aerospace[23]. SMA thin film is considered as a core technology for actuation of MEMS devices, where large force and stroke are essential in conditions of low duty cycles or intermittent operation and in extreme environment such as radioactive, space, biological and corrosive conditions[24]. However, the hysteresis, response speed and precise motion control are the potential problems associated with SMA thin film towards the development of micro devices.

Usually, the SMA will be deposited as a thin film on rigid substrate and peeled off after deposition to enable the development of devices[25-29]. Subsequently, shape training of the SMA thin film is required before deployment. However, the free standing SMA thin films are unable to produce large actuation force. To eliminate the tedious training and to increase the force produced, the SMA thin film was deposited over the flexible substrates. Ishida[30-33], *et al.* have developed a SMA NiTi bimorph and investigated its suitability as micro flapper. Kotnur[34-35], *et al.* have studied the influence of various parameters on NiTi SMA bimorph. Copper based shape memory alloys exhibits a low hysteresis along with interesting electrical and thermal properties. Our research group has developed different types of NiTi and Cu based SMA bimorph actuators using thermal and electron beam evaporation technique[36-41]. Detailed investigations on the influence of substrate temperature on the materials properties and performance of actuators have been reported. Furthermore, the actuation behaviour of the developed copper based SMA bimorph has been evaluated towards its suitability as micro flappers in aerial robots. The attractive actuation behaviour coupled with better life cycle characteristics has enabled the copper based bimorph as the viable candidate for micro mechatronics and micro robotics applications. It was found that the addition of Mn to CuAlNi thin film has significantly increased the life cycles of the SMA bimorph. Because of the higher life cycles, it can be used as an efficient MEMS actuator with larger load capacity for developing low cost and efficient micro devices. Bimorph is a composite structure with films grown over the passive flexible substrate. The bimorph provides two way shape memory effect without any additional bias mechanism.

To utilise these copper-based SMA bimorph in real time, it is essential to have a precise control of the motion. Researchers have developed various linear and non-linear control techniques

Received : 25 February 2020, Revised : 10 June 2020
Accepted : 17 July 2020, Online published : 12 October 2020

for controlling SMA spring and wire based systems[42]. PID controller is the widely used method to control the position of the SMA actuators[43-44]. To the best of author's knowledge, there is no work reported on the control of SMA thin film bimorph actuator. Controlling the motion of SMA bimorph actuator paves way for the development of SMA based micro devices. In this paper, the CuAlNiMn SMA bimorph actuator has been developed and an attempt has been made to control the motion with proper gain tuning. A proportional integral derivative (PID) controller has been designed and implemented to control the displacement of the bimorph actuator. The actuation characteristics of SMA bimorph actuator with respect to displacement, input voltage and load have been investigated. A preliminary prototype of the SMA bimorph actuator based micro positioning system has been developed.

2. METHODOLOGY

2.1 Development of SMA Bimorph Actuator

CuAlNiMn thin film of thickness 2 µm was deposited on kapton polyimide (flexible substrate) using thermal evaporation technique. The kapton polyimide substrate was cleaned and baked before deposition. The polyimide was prestrained and placed in the substrate holder. The source material CuAlNiMn pellet of weight 1 g was placed in the tungsten crucible and evaporated to form the thin film over the polymide substrate. During deposition, the vacuum pressure of 5×10^{-5} mbar was maintained in the chamber. Thin films were fabricated on different substrate thicknesses viz. 25 µm, 50 µm and 75µm. Figure 1 shows the developed SMA bimorph actuator with different substrate thickness. The SMA film thickness was kept constant throughout the work and the substrate thickness has been varied.

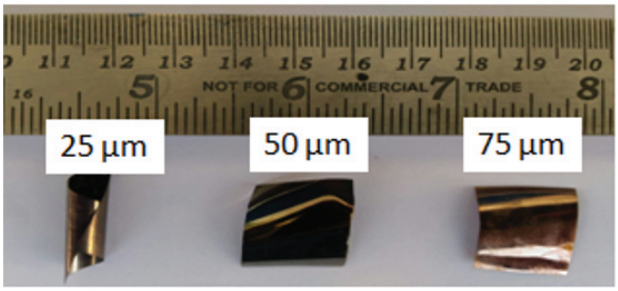

Figure 1. Developed bimorph with different substrate thickness.

Energy dispersive spectroscopy was used to analyze the composition of the thin film. The phase transformation temperature was identified using differential scanning calorimetry (DSC). The phase transformation temperature of CuAlNiMn bimorph after deposition was found to be austenite start (A_s) = 221 °C and austenite finish (A_f) = 235 °C as shown in Fig. 2. There was no evidence of martensite transformation during cooling cycle for the samples. The absence of transformation peak might be due to the effect of the polyimide substrate, which might affect the cooling rate. The atomic composition of CuAlNiMn SMA bimorph is given in Table 1.

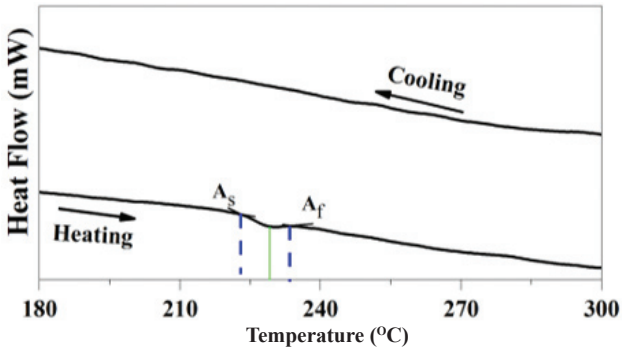

Figure 2. DSC plot of CuAlNiMn.

Table 1. Composition of CuAlNiMn Bimorph

Element	Composition (at. %)
Cu	66.90
Al	25.85
Ni	3.2
Mn	4.01

2.2 Experimental Setup for Actuation and Motion Control

The schematic of the experimental setup is shown in Fig. 3. A laser displacement sensor (LDS) was used to measure the tip displacement of the bimorph and interfaced with LabVIEW software through a data acquisition (DAQ) Agilent 34970A system.

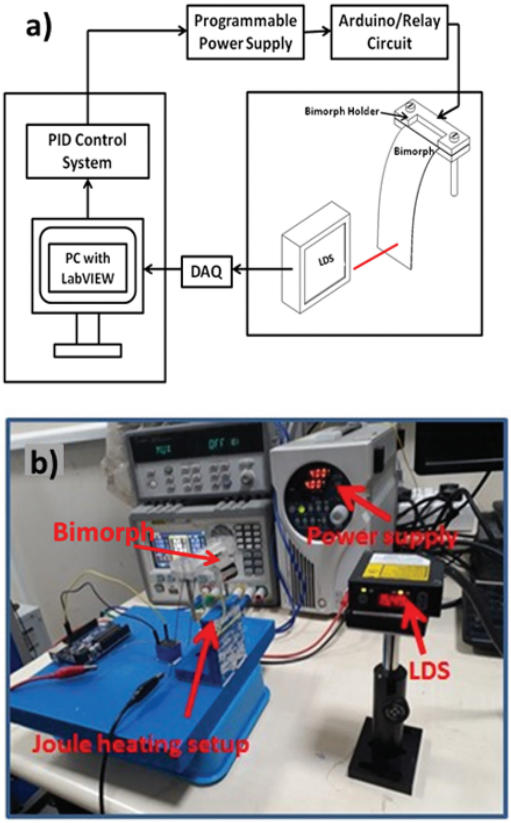

Figure 3. Experimental setup: (a) Schematic image and (b) Actual image.

The SMA can be actuated using different actuation methods such as hot water actuation, electrical actuation[45]. In this work, the bimorph was actuated through electrical actuation (Joule heating) and the input to the bimorph was fed using RIGOL programmable power supply with an Arduino based relay circuit. The resolution of DAQ and LDS are 12.5 ns and 2.5 µm, respectively.

2.3 Controller Design

Proportional integral derivative is a method based on the control loop feedback. PID controller can be understood as a controller that takes the present, the past, and the future of the error into consideration. The PID control equation is given as

$$u(t) = K_p * e + K_i * \int_0^t e dt + K_d * \frac{de}{dt} \quad (1)$$

where $u(t)$ = displacement, e = error, K_p = proportional gain, K_i = Integral gain, K_d = derivative gain. Error e = D_d - D_a (D_d = desired displacement (set point) and D_a = actual displacement). The schematic block diagram of the PID controller design used for the SMA bimorph is shown in Fig. 4. The PID controller was designed in LabVIEW platform. The desired set point is given through the front panel of the LabVIEW. The actual displacement of the bimorph was measured using LDS. The difference between desired displacement and actual displacement is the displacement error e which will be further fed into the PID control equation.

The final displacement correction $u(t)$ is fed into the SMA bimorph through programmable power supply and Arduino with relay circuit. The controller gain is adjusted and tuned accordingly to minimize the error to zero. The PID control module in LabVIEW was fed with preliminary study data of bimorph actuation. The voltage fed into the bimorph is controlled through programmable power supply. The voltage with stipulated time is the control signal fed to the SMA bimorph. The LabVIEW acts as main controller and Arduino acts as slave controller. The Arduino was interfaced with LabVIEW through Interface for Arduino (LIFA).

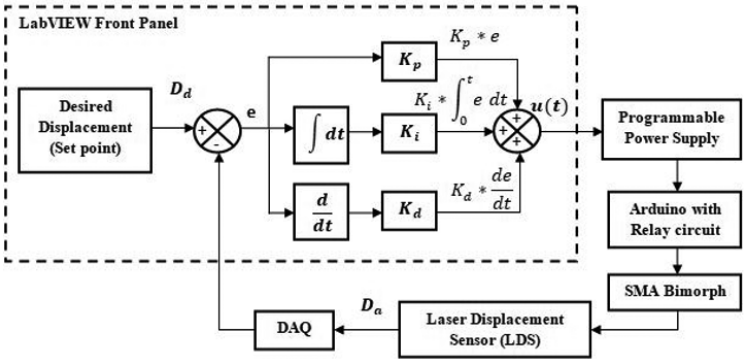

Figure 4. Block diagram of PID control of SMA bimorph actuator.

3. RESULTS AND DISCUSSION

3.1 Actuation Capability of SMA Bimorph Actuator

SMA bimorph actuator with varying substrate thickness (75 µm, 50 µm and 25 µm) have been used for the analysis. The sample size considered for the experiment was 2 cm × 3 cm.

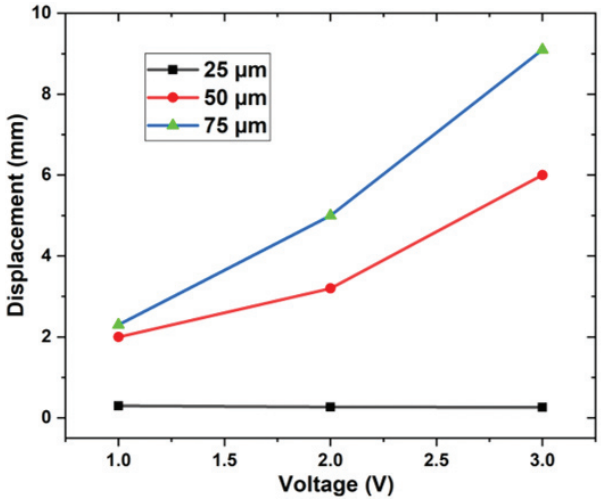

Figure 5. Voltage *vs* displacement curve with different substrate thickness.

Figure 5 shows the maximum displacement of bimorph with respect to varying voltage and different substrate thickness. The voltage was applied until the SMA bimorph moves from initial position to the maximum position (i.e. until it stops moving)and the corresponding displacement was considered as maximum displacement.

It can be clearly observed that the bimorph with substrate thickness 75 µm shows higher displacement than the others. During deposition, the material vapour will transfer some thermal energy to the substrate. Due to this, the thinnest substrate (25 µm) swirls more after deposition (Fig. 1). Because of the lower stiffness of 25 µm and 50 µm substrate, it was unable to counteract the compressive thermal stress induced by SMA film on substrate upon deposition. The radius of curvature is higher for bimorph with lesser substrate thickness. When the substrate thickness increases, the bimorph stiffness get increased and it can easily counterpart the thermal compressive stress induced by SMA thin film. This could be the reason for the higher displacement with respect to increased substrate thickness.

Hence, the SMA bimorph actuator having 75 µm substrate thickness was utilized for further investigations. The actuation characteristics with respect to displacement and voltage have been performed. The bimorph displacement was measured for 2 V and 3 V and plotted in Fig. 6. It can be observed that a maximum of 9 mm was achieved at 3 V.

As a part of thermo-mechanical analysis through Joule heating, displacement under different loads has been carried out. The SMA bimorph was considered as a cantilever beam. One end of the bimorph is fixed in the bimorph holder and load has been attached to the other end. The load has been varied as 30 mg, 45 mg and 60 mg for the investigation. Figure 7 shows the maximum displacement with varying loads. It is evident that the bimorph can be actuated with load and extended for MEMS application.

3.2 Control of the Bimorph

An initial test has been performed to find the input range

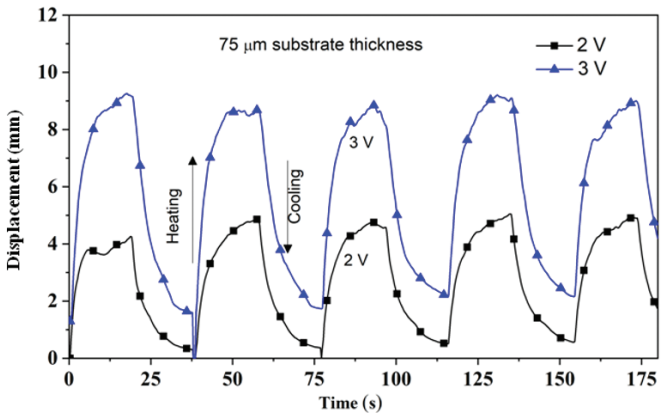

Figure 6. Time vs. displacement curve for 2 V and 3 V.

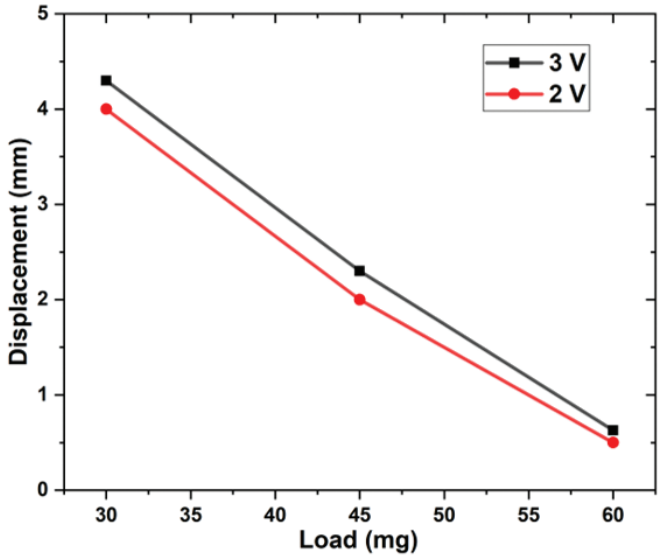

Figure 7. Maximum displacement with different loads.

at which the displacement of bimorph occurs. The bimorph started actuating between an input range of 0-3 V. The operating range has been given to the PID module output in the LabVIEW environment. Initially the PID controller gain parameters are tuned based on trial and error method. A set point displacement control has been done to find out the critical gain. The bimorph control has been performed to know the critical gain values region where the system is stable. The gain value K_p increased until the displacement reached the set point, K_i increased to decrease the precision error and K_d was increased to reduce the overshoot. In trial and error based method different gain values generated quasi-semi stability of displacement to reach desired set point position. It has been observed that the gain K_p = 9.5 produce less oscillation and achieved stable displacement compared to other gain values. The proportional gain value has been varied from 0 to 9.8. The integral gain value has been varied from 2.5-3.2. The derivative gain value has been varied from 2.7-3.3. For integral gain, above these ranges the system showed more oscillation. For derivative gain, above these ranges the system could not reach the set point. Integral absolute error (IAE) has been calculated for different gain values and tabulated as shown in Table 2.

Table 2. Cumulative error for various proportional gain

Proportional gain	IAE (m)
9	0.08298
9.5	0.01497
9.75	0.0823
9.74	0.09476
9.76	0.0847
9.78	0.07864
9.82	0.07678
9.85	0.08713
9.8	0.07469

The set point 0.5 mm is again tested with the gain values and plotted in Fig. 8. Here the error comparing to set point was more and has more peaks. The controller needs to be tuned more precisely to reach the desired set point with less fluctuation, minimum error and stability.

Based on the critical gain values the controller was designed using standard Zeigler Nichol's (Z-N) method[46]. In Z-N method, increasing the K_p value from 0 to a critical value K_{cr} = 9.8 exhibited sustained oscillations. The corresponding critical period value P_{cr} = 4 have been determined experimentally. Based on the K_{cr} and P_{cr} values, the proportional gain K_p, integral gain K_i and derivative gain K_d have been found using Z-N tuning rule. As per Zeigler-Nichol's rule, it was performed by setting the integral and derivative gains to zero. Then the proportional gain was increased from zero until it reaches the ultimate gain or critical gain, at which the output of the control loop has stable and consistent oscillations.

The bimorph stability for the standard Z-N method critical gains is shown in Fig. 9. It can be observed that the system is stable with minimal error. The tuned value of PID controller parameters is K_p=5.88, T_i=2, T_d=0.5. Based on the obtained result using tuned Z-N parameters, it shows that the SMA bimorph motion can be controlled. The error with respect to desired set point is less for CuAlNiMn bimorph and evidences the better control characteristics of CuAlNiMn bimorph. To ensure the same behavior, the bimorph control has been tested for different set points from 0.6 mm to 1 mm at an interval of

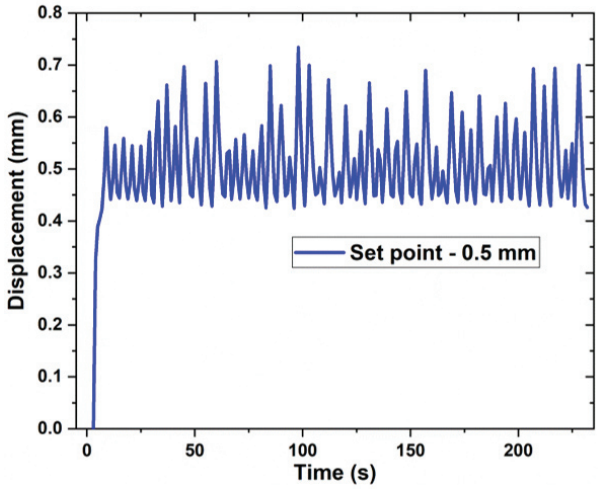

Figure 8. Displacement Stability for gain K_p = 9.5 (set point of 0.5 mm).

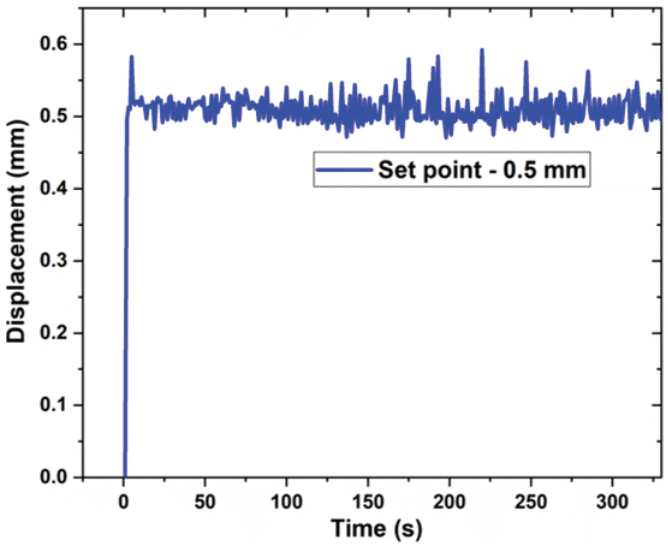

Figure 9. Time vs. Displacement for set point of 0.5 mm using standard parameter Z-N method.

0.1 mm. Figures 10 (a-e) shows the time vs. displacement graph for various desired set point of 0.6 mm to 1 mm. From the results, it was observed that the position of bimorph actuator accurately changes with respect to the desired set point with minimal error and stability. Especially with the tuned Z-N parameters, the oscillations were reduced and the bimorph becomes stable with minimum error. The standard deviation, a 95% confidence interval is 0.793 ± 0.020 (range between 0.793 to 0.813). To achieve precise control with zero error and stability, intelligent control techniques like fuzzy and neural network based control can be adopted in future.

4. PROPOSED APPLICATION

A preliminary prototype of SMA bimorph actuator based micro positioning system has been developed for MEMS applications. The developed micro positioning prototype can be used for manipulating smaller objects with high precision. The developed SMA bimorph actuator based micro positioning system is shown in Fig. 11.

It consists of three SMA bimorph links arranged in a parallel manipulator configuration with one end of each bimorph fixed to the base. The other end of bimorph is attached to the top plate which undergoes micro positioning. By actuating three bimorph links simultaneously, the top plate moved in vertical direction along z axis. During the initial study, it has generated a displacement of 5 mm vertically. The displacement has been measured using LDS and the experimental setup as shown in Fig. 12.

By actuating any two links, a twisting orientation can be achieved. Detailed investigations on micro positioning and control of the proposed SMA bimorph based micro positioning system are under progress.

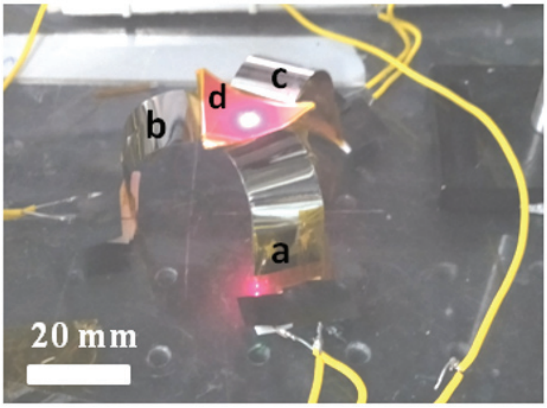

Figure 11. Preliminary prototype of the proposed SMA bimorph actuator based micro positioning system for MEMS applications. (a) Link 1, (b) Link 2 (c) Link 3, and (d) Top plate.

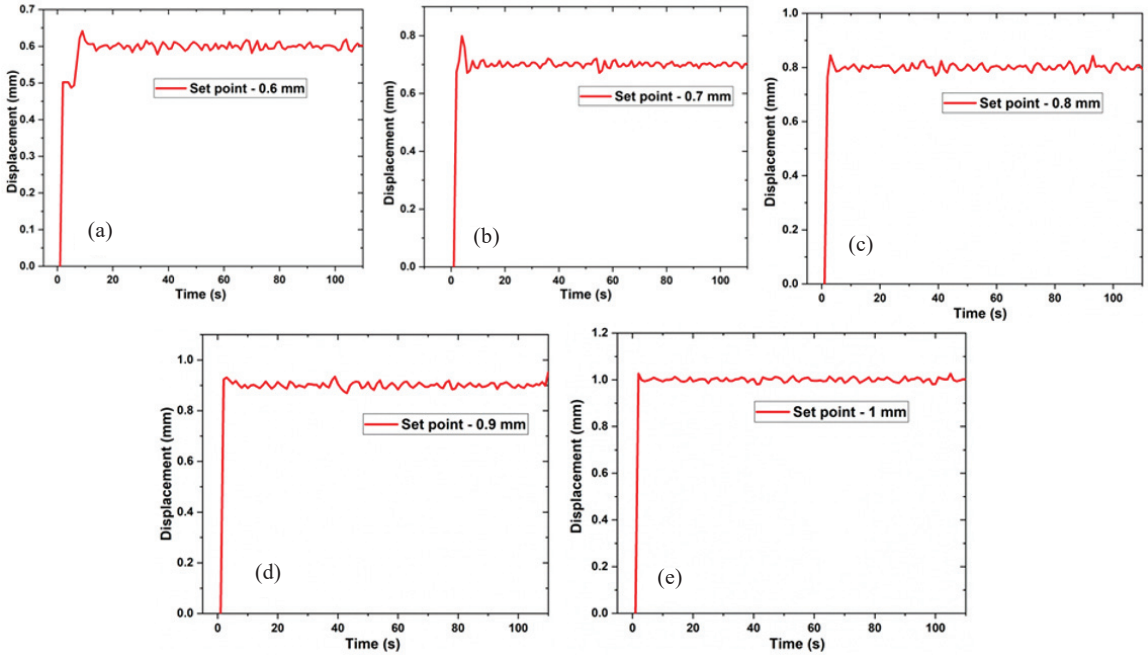

Figure 10. Time vs. Displacement for desired set point of (a) 0.6 mm, (b) 0.7 mm, (c) 0.8 mm, (d) 0.9 mm, and (e) 1 mm.

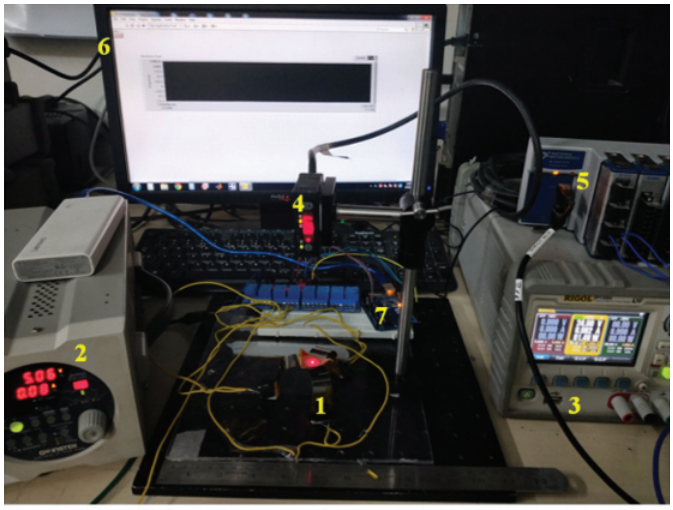

1) SMA Bimorph based stewart platform 2) Power supply for Bimorph 3) Power supply for LDS 4) Laser displacement sensor (LDS) 5) Data acquisition system (DAQ) 6) PC with Lab VIEW 7) Arduino with relay circuit

Figure 12. Experimental Setup of 3D micro positioning system.

5. CONCLUSIONS

CuAlNiMn SMA thin film was successfully fabricated on flexible substrate with different thickness using thermal evaporation technique. The SMA bimorph with 75 µm substrate thickness showed a better performance compared to bimorph with lesser substrate thickness. The actuation characteristics with respect to varying load of 30 mg, 45 mg and 60 mg has been performed and it was evident that the SMA bimorph actuator can be actuated with load. PID controller has been implemented successfully to control the SMA bimorph. The controller gains have been tuned with Zeigler Nichol's method. The results confirmed that the SMA bimorph can be controlled and extended for dedicated MEMS applications. The study will be helpful to control the individual bimorph in the proposed bimorph based micro positioning system.

REFERENCES

1. Meng, Q. & Hu, J. A review of shape memory polymer composites and blends. *Compos. A: Appl. Sci. Manuf.*, 2009, **40**, 1661–1672. doi: 10.1016/j.compositesa.2009.08.011.
2. Tsoi, K.A.; Stalmans, R.; Schrooten, J.; Wevers, M. & Mai, Y.W. Impact damage behavior of shape memory alloy composites. *Mater. Sci. Eng. A.,* 2003, **342**, 207–215. doi: 10.1016/S0921-5093(02)00317-9.
3. Schrooten, J.; Michaud, V. & Parthenios, J. Progress on composites with embedded shape memory alloy wires. *Mater. Trans*., 2002, **43**, 961–973. doi: 10.2320/matertrans.43.961
4. Zardetto, V.; Brown, T.M.; Reale, A. & Di Carlo, A. Substrates for flexible electronics: a practical investigation on the electrical, film flexibility, optical, temperature, and solvent resistance properties. *J. Polym. Sci. B Polym. Phys*., 2001, **49**, 638–648. doi: 10.1002/polb.22227.
5. Tsoi, K.A.; Schrooten, J. & Stalmans, R. Part I. Thermomechanical characteristics of shape memory alloys. *Mater. Sci. Eng. A.,* 2004, **368**, 286–298. doi: 10.1016/j. msea.2003.11.006.
6. Saunders, W.R.; Robertshaw, H.H. & Rogers, C.A. Structural acoustic control of a shape memory alloy composite beam. *J. Intell. Mater. Syst. Struct*., 1991, **2**, 508–527. doi: 10.1177/1045389X9100200406
7. Lester, B.T.; Baxevanis, T.; Chemisky, Y. & Lagoudas, D.C. Review and perspectives: shape memory alloy composite systems. *Acta Mech*., 2015, **226**, 3907–3960. doi: 10.1007/s00707-015-1433-0.
8. Kamalakannan, G.M.; Giresh Kumar Singh. & Ananda, C.M. A Multi-segment Morphing System for a Micro Air Vehicle using Shape Memory Alloy Actuators. *Def. Sc. J.*, 2020, **70**(1), 3-9. doi : 10.14429/dsj.70.14145
9. Yamauchi K, Ohkata I, Tsuchiya K, Miyazaki S. ShapeMemory and Superelastic Alloys Technologies and Applications. Woodhead Publishing, 2011. 232p.
10. Dimitris C. Lagoudas. Shape Memory Alloys: Modeling and Engineering Applications. Springer US, 2008. 436. doi: 10.1007/978-0-387-47685-8.
11. Yang, S.; Zhang, F.; Wu, J.; Lu, Y.; Shi, Z.; Wang, C.& Liu, X. Superelasticity and shape memory effect in Cu–Al–Mn–V shape memory alloys. *Mater. Des*., 2017, **115**, 17–25. doi: 10.1016/j.matdes.2016.11.035.
12. Oliveira, J.P.; Zeng, Z.; Andrei, C.; Braz Fernandes, F.M.; Miranda, R.M.; Ramirez, A.J.; Omori, T.& Zhou, N. Dissimilar laser welding of superelastic NiTi and CuAlMn shape memory alloys. *Mater. Des.,* 2017, **128**, 166–175. doi: 10.1016/j.matdes.2017.05.011.
13. Shariat, B.S.; Meng, Q.; Mahmud, A.S.; Wu, Z.; Bakhtiari, R.; Zhang, J.; Motazedian, F.; Yang, H.; Rio, G.; Nam, T.H.& Liu, Y. Functionally graded shape memory alloys: design, fabrication and experimental evaluation. *Mater. Des*., 2017, **124**, 225–237. doi: 10.1016/j.matdes.2017.03.069.
14. Kim, M.S.; Chu, W.S.; Lee, J.H.; Kim, Y.M. & Ahn, S.H. Manufacturing of Inchworm Robot Using Shape Memory Alloy (SMA) Embedded Composite Structure. *International Journal of Precision Engineering and Manufacturing*., 2011, **12**(3), 565-568. doi: 10.1007/s12541-011-0071-2
15. Liu, T.; Zhou, T.; Yao, Y.; Zhang, F.; Liu, L.; Liu, Y. & Leng, J. Stimulus methods of multifunctional shape memory polymer nanocomposites: a review. *Compos. A: Appl. Sci. Manuf.,* 2017, **100**, 20–30. doi: 10.1016/j.compositesa.2017.04.022.
16. Kim, Y. & Do, D. Shape memory characteristics of highly porous Ti-rich TiNi alloys. *Mater. Lett.*, 2016, **162**, 1–4. doi: 10.1016/j.matlet.2015.09.101.
17. Gugel, H.; Schuermann, A. & Theisen, W. Laser welding of NiTi wires. *Mater. Sci. Eng. A.,* 2008, **481–482**, 668–671. doi: 10.1016/j.msea.2006.11.179.

18. Huang, X. & Liu, Y. Surface morphology of sputtered NiTi-based shape memory alloy thin films. *Surf. Coat. Technol.,* 2005, **190**, 400–405. doi: 10.1016/j. surfcoat.2004.02.029.
19. Gill, J.J.; Chang, D.T.; Momoda, L.A. & Carman, G.P. Manufacturing issues of thin film NiTi micro wrapper. *Sens. Actuators A Phys.,* 2001, **93**, 148–156. doi: 10.1016/S0924-4247(01)00646-X.
20. Shin, D.D.; Lee, D.G.; Mohanchandra, K.P. & Carman, G.P. Thin film NiTi microthermostat array. *Sens. Actuators A Phys.,* 2006, **130–131**, 37–41. doi: 10.1016/j.sna.2005.10.010
21. Sassa, F.; Al-Zain, Y.; Ginoza, T.; Miyazaki, S. & Suzuki, H. Miniaturized shape memory alloy pumps for stepping microfluidic transport. *Sens. Actuators B Chem*., 2012, **165**, 157–163. doi: 10.1016/j.snb.2011.12.085
22. Shin, D.D.; Mohanchandra, K.P. & Carman, G.P. High frequency actuation of thin film NiTi. *Sens. Actuators A Phys.,* 2004, **111**, 166–171. doi: 10.1016/j.sna.2003.09.026
23. Choudhary, N. & Kaur, D. Shape memory alloy thin films and heterostructures for MEMS applications: A review. *Sens. Actuators A Phys.,* 2016, **242**, 162–181. doi: 10.1016/j.sna.2016.02.026
24. Fu, Y.Q.; Luo, J.K.; Flewitt, A.J.; Huang, W.M.; Zhang, S.; Du, H.J. & Milne, W.I. Thin film shape memory alloys and micro actuators. *Int. J. Comput. Mater. Sci.Surface Eng.*, 2009, Vol. **2**, Nos. 3/4. doi: 10.1504/IJCMSSE.2009.027483
25. Huang, X.; San Juan, J. & Ramirez, A.G. Evolution of phase transformation behavior and mechanical properties with crystallization in NiTi thin films. *Scripta Materialia.,* 2010, **63**, 16–19. doi: 10.1016/j.scriptamat.2010.02.037
26. Kotnur, V.G. & Janssen, G.C.A.M. In situ stress measurements and mechanical properties of a composition range of NiTi thin films deposited at elevated temperature. *Surface Coatings Technol*., 2012, **211**, 167–171. doi: 10.1016/j.surfcoat.2011.10.047
27. Sanjabi, S. & Barber, Z.H. The effect of film composition on the structure and mechanical properties of NiTi shape memory thin films. *Surface Coatings Technol*., 2010, **204**, 1299–1304. doi: 10.1016/j.surfcoat.2009.10.013
28. Wang, X. & Joost J. Vlassak. Thickness and film stress effects on the martensitic transformation temperature in equi-atomic NiTi thin films. *Mechanics Materials.,* 2015, **88**, 50–60. doi: 10.1016/j.mechmat.2015.05.001
29. Tillmann, W. & Momeni, S. Tribological performance of near equiatomic and Ti-rich NiTi shape memory alloy thin films. *Acta Materialia*., 2015, **92**, 189–196. doi: 10.1016/j.actamat.2015.04.006
30. Ishida, A. Ti–Ni–Cu/polyimide composite-film actuator and simulation tool. *Sens. Actuators A: Phys.*, 2015, **222**, 228–236. doi:10.1016/j.sna.2014.12.012.
31. Ishida, A. & Sato, M. Ti-Ni-Cu shape-memory alloy thin film formed 356 on polyimide substrate. *Thin Solid Films.*, 2008, **516**, 7836–7839. doi:10.1016/j.tsf.2008.04.091.
32. Ishida, A. & Sato, M. Development of Polyimide/SMA Thin-Film Actuator. *Mater. Sci. Forum*., 2010, **654–656**, 2075–2078. doi:10.4028/www.scientific.net/MSF.654-656.2075.
33. Ishida, A. & Martynov, V. Sputter-deposited alloy thin films: Properties and applications. *MRS Bull.*, 2002, **27**(2), 111–114. doi: 10.1557/mrs2002.46
34. Kotnur, V.G.; Tichelaar, F.D.; Fu, W.T.; De Hosson, J.T.M. & Janssen, G.C.A.M. Shape memory NiTi thin films deposited at low temperature. *Surf. Coatings Technol*., 2014, **258**, 1145–1151. doi:10.1016/S0921-5093(99)00403-7.
35. Kotnur, V.G.; Tichelaar, F.D. & Janssen, G.C.A.M. Sputter deposited Ni-Ti thin films on polyimide substrate, *Surf. Coatings Technol.*, 2013, **222**, 44–47. doi:10.1016/j.surfcoat.2013.01.058.
36. Akash, K.; Jain, A.K.; Karmarkar, G.; Jadhav, A.; Narayane, D.C.; Patra, N. & Palani, I.A. Investigations on actuation characteristics and life cycle behaviour of CuAlNiMn shape memory alloy bimorph towards flappers for aerial robots. *Materials and Design.*, 2018, **144**, 64–71. doi: 10.1016/j.matdes.2018.02.013
37. Akash, K.; Mani Prabu, S.S.; Shukla, A.K.; Nath, T.; Karthick, S. & Palani, I.A. Investigations on the life cycle behavior of Cu-Al-Ni/polyimide shape memory alloy bi-morph at varying substrate thickness and actuation conditions. *Sensors and Actuators A.*, 2017, **254**, 28–35. doi: 10.1016/j.sna.2016.12.008
38. Akash, K.; Shukla, A.K.; Mani Prabu, S.S.; Narayane, D.C.; Kanmanisubbu, S. & Palani, I.A. Parametric investigations to enhance the thermomechanical properties of CuAlNi shape memory alloy Bi-morph. *J. Alloys Compounds*, 2017, **720**, 264-271. doi: 10.1016/j.jallcom.2017.05.255
39. Akash, K.; Mani Prabu, S.S.; Gustmann, T.; Jayachandran, S.; Pauly, S. & Palani, I.A. Enhancing the Life Cycle Behaviour of Cu-Al-Ni Shape Memory Alloy bimorph by Mn Addition. *Materials Letters*, 2018, 226, 55-58. doi: 10.1016/j.matlet.2018.05.008.
40. Jayachandran, S.; Akash, K.; Mani Prabu, S.S.; Manikandan, M.; Muralidharan, M.; Brolin, A. & Palani, I.A. Investigations on performance viability of NiTi, NiTiCu, CuAlNi and CuAlNiMn shape memory alloy/ Kapton composite thin film for actuator application. *Composites Part B: Eng.*, 2019, **176**, 107182. doi: 10.1016/j.compositesb.2019.107182
41. Jayachandran, S.; Mani Prabu, S.S.; Manikandan, M.; Muralidharan, M.; Harivishanth, M.; Akash, K. & Palani, I.A. Exploring the functional capabilities of NiTi shape memory alloy thin films deposited using electron beam evaporation technique. *Vacuum*, 2019, **168**, 108826. doi: 10.1016/j.vacuum.2019.108826
42. Sreekumar, M.; Singaperumal, M.; Nagarajan, T.; Zoppi,

M. & Molfino. Recent advances in nonlinear control technologies for shape memory alloy actuators. *J. Zhejiang. Univ. Sci. A*., 2007, **8**(5), 818-829. doi: 10.1631/jzus.2007.A0818

43. Álvaro Villoslada.; Naiara Escudero.; Fernando Martín.; Antonio Flores.; Cayetano Rivera.; Marcelo Collado. & Luis Moreno. Position control of a shape memory alloy actuator using a four-term bilinear PID controller. *Sens. Actuat., A: Phy*., 2015, **236**, 257–272. doi: 10.1016/j.sna.2015.10.006
44. Li, J. & Tian, H. Position control of SMA actuator based on inverse empirical model and SMC-RBF compensation. *Mech. Sys. Signal Proc.*, 2018, **108**, 203–215. doi: 10.1016/j.ymssp.2018.02.004
45. Nath, T.; Chouhan, P.; Disawal, R. & Palani, I.A. Comparative study of electrically and hot water actuated shape memory alloy using thermo-mechanical cycle test bench. *Def. Sci. J.*, 2017, **67(**1), 100-107. doi : 10.14429/dsj.67.10489
46. Ziegler, J.G. & Nichols, N.B. Optimum settings for automatic controllers, *Trans. ASME*, 1942, **64**, 759-768.

ACKNOWLEDGEMENT

The authors would like to thank Dr Devendra Deshmukh, Mechanical Engineering, IIT Indore for providing the LabVIEW facility to perform the experimentation.

CONTRIBUTORS

Mr M. Muralidharan received his BE and ME in Mechatronics from Kongu Engineering College. Currently, he is a Research Scholar in Mechatronics and Instrumentation Laboratory, Department of Mechanical Engineering, Indian Institute of Technology Indore. His broad area of research interests includes mechatronics, soft robotics, bio-inspired robotics and smart materials.
In the present study, he is involved in fabrication, experimentation, prototype development and paper writing.

Mr S. Jayachandran received his Master's from PSG College of technology. Currently, he is a Research Scholar in Mechatronics and Instrumentation Laboratory, Department of Mechanical Engineering, Indian Institute of Technology Indore. His broad area of research interests includes smart materials and thin films.
In the present study, he has coordinated in the fabrication and actuation characteristics of SMA Bimorph.

Mr M. Yogeshwaran has completed his BE (Mechatronics) from Bannari Amman Institute of Technology and served as project intern at Mechatronics and Instrumentation Laboratory, Department of Mechanical Engineering, Indian Institute of Technology Indore.
In the present study, he has coordinated in the experimentation and control studies.

Ms A.S. Shivaani has completed her BE (Mechatronics) from Bannari Amman Institute of Technology and served as project intern at Mechatronics and Instrumentation Laboratory, Department of Mechanical Engineering, Indian Institute of Technology Indore.
In the present study, she has coordinated in the experimentation and control studies.

Dr I.A. Palani received his PhD from Department of Mechanical Engineering, IIT Madras, India. He was a Post-Doctoral Fellow in Graduate School of Information Science and Electrical Engineering, Kyushu University, Japan. Presently working as an Associate Professor and heading the Mechatronics and Instrumentation Laboratory at Indian Institute of Technology Indore. His area of interest includes laser-assisted micro processing, surface engineering, opto-mechatronics, soft robotics, smart materials and nano structures for functional device.
In the present study, he is involved in conceptualization, resource and funding, review, editing and project leader.